Novel Strategy for Assigning Hyperfine Shifts Using Pulsed-Field Gradient Heteronuclear Multiple-Bond Correlation Spectroscopy†

Ken Skidmore and Ursula Simonis*

Department of Chemistry and Biochemistry, San Francisco State University, San Francisco, California 94132

Received July 10, 1996

Our interest in delineating the unpaired electron spin density distribution within the porphyrin π orbitals of low-spin iron(III) porphyrins[1] has led us to use pulsed-field gradient (PFG) techniques[2−8] to assess their overall value for assigning hyperfine shifts in the NMR spectra of these paramagnetic complexes and for detecting low-intensity cross peaks. This paper illustrates the advantages of using gradient pulses for the acquisition of a two-dimensional (2D) proton-detected heteronuclear multiple-bond correlation spectroscopy (HMBC) map of the bis(*N*-methylimidazole) complex of (5-(*o*-nitrophenyl)-10,15,20-triphenylporphyrinato)iron(III), **1**. It shows for the first time that HMBC using gradient coherence-transfer selection (PFG HMBC)[2−8] provides a novel and powerful approach for obtaining long-range ^{1}H−^{13}C couplings of paramagnetic complexes.

Although 2D NMR spectroscopy has been used successfully for assigning the NMR spectra of paramagnetic complexes,[1,9,10] unambiguous ^{1}H and ^{13}C hyperfine shift assignments have only been accomplished for a few proteins and model complexes.[1b,11−14] Due to the short relaxation times, the spin systems relax to their equilibrium position during the course of the NMR experiment. Thus, transfer of magnetization or coherence between sets of spins is small, and cross peak intensity is diminished or lost. Most often it is rather difficult to pull such weak responses out of the t_1 noise level.[1,12−15]

Recently, it was shown that the use of pulsed-field gradients for coherence-transfer selection significantly reduces t_1 artifacts in multidimensional NMR maps of diamagnetic molecules, since only the magnetization pathway of interest is selected. Phase cycling is eliminated, so that there is no reliance on subtraction of unwanted signal.[2−7] However, relative to the conventional phase-cycled experiment, the signal-to-noise ratio of the peaks in PFG spectra is lowered by a factor of $\sqrt{2}$, because only one of the two magnetization-transfer pathways, which normally contribute to the observed signal, is refocused.[2,4,6] Furthermore, gradient pulses add to the length of the pulse sequence, thereby increasing the potential for T_2 relaxation. Nevertheless, we will show below that, in spite of these disadvantages, PFGs provide major improvements for the detection of long-range ^{1}H−^{13}C connectivities in HMBC maps of paramagnetic molecules, suggesting that the significant decrease in t_1 artifacts outweighs the magnetization loss due to relaxation. Consistent with this is our recent finding that the use of gradient pulses similarly facilitates the detectability of ^{1}H−^{1}H cross peaks in COSY maps of other paramagnetic iron porphyrin complexes.[15] The potential of the PFG HMBC experiment[3c] is illustrated for a 25 mM $CDCl_3$ sample of **1**. The PFG HMBC maps of **1** at 302 K are shown in Figure 1b,c together with the structure of the complex (Figure 1a) and the 1D ^{1}H and ^{13}C NMR spectra on the axes. For reasons of clarity, the phenyl C resonances at 125−150 ppm are not shown in the ^{13}C NMR spectrum.

As can be seen in the ^{13}C NMR spectrum of **1** (Figure 1b), the resonances most shifted by the interaction of the unpaired electron of low-spin iron(III) are those of the pyrrole α- and β-carbons and the *meso*-C's of the methine bridges, which, at 302 K, resonate in the spectral region 30−120 ppm. The four pyrrole β-C signals downfield from $CDCl_3$ are easily identified by the chemical shift correlations linking the pyrrole β-C to the directly bonded protons using the conventional ^{13}C-detected HETCOR[16] experiment.[17] It should be noted that these $^1J_{CH}$ correlations are also observed in the gradient HMBC map of the complex, as is evidenced by the cross peaks in the boxed area of Figure 1c. The pyrrole α-carbons and the *meso*-carbons of **1** give rise to a total of seven upfield-shifted resonances in the narrow spectral range of 30−60 ppm. At 302 K, two of the expected eight signals overlap and one of the resonances is masked by the methyl carbon signal of free *N*-MeIm (*N*-methylimidazole) at 33.8 ppm. For bound *N*-MeIm, this methyl C resonates at 23.8 ppm, which is confirmed by the cross peak linking the ^{13}C resonance at 23.8 ppm to the downfield-shifted ^{1}H methyl signals of bound *N*-MeIm at 21 ppm.

To assign the α- and *meso*-C resonances, it was essential to use ^{1}H-detected heteronuclear multiple-bond correlation spectroscopy, since ^{13}C-detected methods[18−20] failed to provide the desired couplings due to the low sensitivity of these experiments

† This work was presented as a poster at the 37th Experimental Nuclear Magnetic Resonance Conference, Pacific Grove, CA, March 1996.

(1) (a) Walker, F. A.; Simonis, U. In *Biological Magnetic Resonance: NMR of Paramagnetic Molecules*; Berliner, L. J., Ruben, J., Eds.; Plenum Press: New York, 1993; Vol. 12, p 133. (b) Tan, H.; Simonis, U.; Shokhirev, N. V.; Walker, F. A. *J. Am. Chem. Soc.* **1994**, *116*, 5784.
(2) Keeler, J.; Clowes, R. T.; Davis, A. L.; Laue, E. D. In *Methods in Enzymology*; James, T. L., Oppenheimer, N. J., Eds.; Academic Press: New York, 1994; Vol. 239, p 145.
(3) (a) Hurd, R. E. *J. Magn. Reson.* **1990**, *87*, 422. (b) Hurd, R. E.; John, B. K. *J. Magn. Reson.* **1991**, *92*, 658. (c) Hurd, R. E.; John, B. K. *J. Magn. Reson.* **1991**, *91*, 648.
(4) Kay, L. E. *Curr. Opin. Struct. Biol.* **1995**, *5*, 674.
(5) (a) Sattler, M.; Schwendinger, M. G.; Schleucher, J.; Griesinger, C. *J. Biomol. NMR* **1995**, *5*, 11. (b) Schleucher, J.; Schwendinger, M.; Sattler, M.; Schmidt, P.; Schedletzky, O.; Glaser, S. J.; Sørensen, O. W.; Griesinger, C. *J. Biomol. NMR* **1994**, *4*, 301.
(6) Zuiderweg, E. R. P.; Majumdar, A. *Trends Anal. Chem.* **1994**, *13*, 73.
(7) Price, W. S. *Annu. Reports NMR Spectrosc.* **1996**, *30*, 53.
(8) Dalvitt, C.; Young Ko, S.; Böhlen, J. M. *J. Magn. Reson.* **1996**, *B110*, 124.
(9) La Mar, G. N.; de Ropp, J. S. In *Biological Magnetic Resonance: NMR of Paramagnetic Molecules*; Berliner, L. J., Ruben, J., Eds.; Plenum Press: New York, 1993; Vol. 12, p 1.
(10) Bertini, I.; Turano, P.; Vila, A. J. *Chem. Rev.* **1993**, *93*, 2833.
(11) Timkovich, R. *Inorg. Chem.* **1991**, *30*, 37.
(12) (a) Turner, D. L. *Eur. J. Biochem.* **1995**, *227*, 829. (b) Banci, L.; Pieratelli, R.; Turner, D. L. *Eur. J. Biochem.* **1995**, *232*, 522. (c) Turner, D. L. *Eur. J. Biochem.* **1993**, *211*, 563.
(13) Clark, K.; Dugad, L. B.; Bartsch, R. G.; Cusanovich, M. A.; La Mar, G. N. *J. Am. Chem. Soc.* **1996**, *118*, 4654.
(14) Yamamoto, Y. *FEBS Lett.* **1987**, *222*, 115.
(15) Marquez, J.; Simonis, U.; Deese, A. *Book of Abstracts*, 37th Experimental Nuclear Magnetic Resonance Conference, Pacific Grove, CA, 1996; p 124.
(16) (a) Bax, A.; Sarkar, S. K. *J. Magn. Reson.* **1983**, *60*, 170. (b) Bodenhausen, G.; Freeman, R. *J. Am. Chem. Soc.* **1978**, *100*, 320.
(17) Tan, H. M.S. Thesis, San Francisco State University, May 1994.
(18) Kessler, H.; Gerke, M.; Griesinger, C. *Angew. Chem., Int. Ed. Engl.* **1988**, *27*, 490.
(19) Zektzer, A. S.; John, B. K.; Martin, G. E. *Magn. Reson. Chem.* **1987**, *25*, 752.
(20) Krishnamurthy, V. V.; Nunlist, R. *J. Magn. Reson.* **1988**, *80*, 280.

S0020-1669(96)00797-5 CCC: $12.00

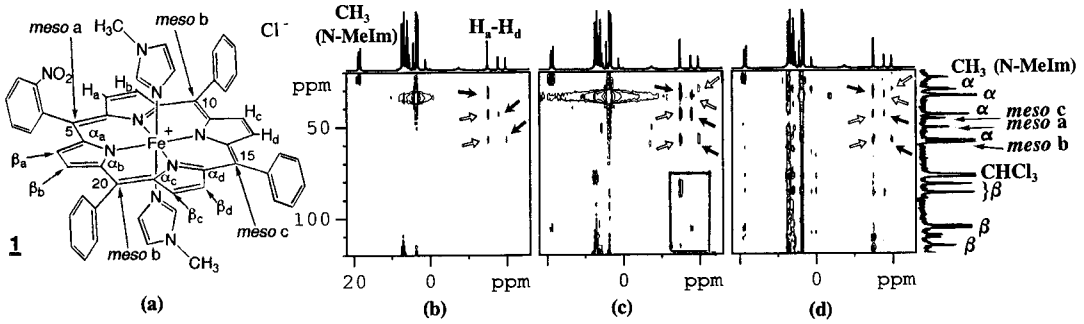

Figure 1. (a) Molecular structure of **1**. (b−d) HMBC maps of a 25 mM solution of **1** in $CDCl_3$ at 302 K acquired on a 299.92 MHz Bruker Avance DRX spectrometer with (b) pulsed-field gradients and 1024 transients per FID, (c) pulsed-field gradients and 8192 transients per FID, and (d) phase-cycling and 8192 transients per t_1 increment. The 2D data for all maps were recorded in the proton dimension with a spectral width of 15 625 Hz, 2048 t_1 increments, and a 11.3 μs 90° pulse width. In the carbon dimension, a spectral width of 13576 Hz, a 14.6 μs 90° pulse, and 64 FIDs were used to give total acquisition times of 3.5 h for (b), 29.5 h for (c), and 28.9 h for (d). For (b) and (c) sine-shaped pulsed-field gradient pulses of 1 ms duration, a pulse ratio of 50:30:40, and strengths of 15, 9, and 12 G/cm were used. The data were multiplied with a phase-shifted sine-squared window function in f_2 and a sine function in f_1 prior to Fourier transformation. The cross peaks marked with solid arrows are due to two-bond pyrrole β-H−pyrrole α-C correlations, and those marked with open arrows are due to $^3J(^1H_\beta-^{13}C_\alpha)$ couplings. The cross peaks in the boxed area of Figure 1c are due to nonsuppressed one-bond scalar correlations linking the pyrrole β-H to the pyrrole β-C signals.

and the short ^{1}H and ^{13}C relaxation times of the complex (proton $T_2 < T_1 < 12$ ms; carbon $T_2 < T_1 < 45$ ms). Proton detection was therefore employed, and HMBC[21] and PFG HMBC[22] maps of **1** were acquired. To successfully obtain the desired two- and three-bond heteronuclear scalar coupling information in both the gradient and nongradient HMBC maps, it was necessary to (a) use a delay ($1/^2J_{CH}$) of 25 ms, (b) acquire the gradient HMBC map with 1024 transients per FID, leading to a total acquisition time of 3.5 h, and (c) record the phase-cycled HMBC map with 8192 transients per t_1 increment (≈29 h). The PFG and nongradient HMBC spectra are shown in Figure 1, parts b and d, respectively. To clearly portray the advantages of the gradient HMBC experiment, the PFG HMBC map, acquired with 8192 scans per FID, is shown in Figure 1c.

The PFG HMBC map in Figure 1b reveals strong cross peaks due to two-bond couplings between the pyrrole β-protons and the pyrrole α-carbons resonating at 58.0, 44.2, 33.8, and 30.4 ppm. These correlations are marked with solid arrows in the figure. Due to the low resolution in the ^{13}C dimension, the cross peaks between the most downfield pyrrole β-H and the two most upfield pyrrole α-C signals are not resolved. The observations of the $^2J(^1H_\beta-^{13}C_\alpha)$ chemical shift correlations identified the hyperfine-shift positions of the four pyrrole α-carbons in **1** and allowed the resonances at 59.5, 51.2, and 46.3 ppm of relative intensities of 2:1:1 to be classified as the *meso*-C's by default, since they are the only peaks that remained unidentified in the spectral region 30−60 ppm. To verify this assignment and exclude the possibility that the above cross peaks arise from $^3J_{CH}$ between the pyrrole β-H and the *meso*-C, the complex with three *meso* positions enriched by ^{13}C to about 10% was synthesized. Only the *meso*-C attached to the substituted phenyl ring remained at natural abundance. This enrichment enabled us to ascertain the resonance positions of the *meso*-carbon atoms with *meso*-C (c) resonating at 46.3 ppm, *meso*-C (b) at 59.5 ppm, and *meso*-C (a) at 51.2 ppm.[23]

In addition to the $^2J_{CH}$ couplings, cross peaks between two pyrrole H's and pyrrole α-C's, marked with open arrows, are observed in the gradient HMBC map in Figure 1b. These chemical shift correlations are due to three-bond couplings between the pyrrole β-H and pyrrole α-C atoms. To observe the remaining two $^3J(^1H_\beta-^{13}C_\alpha)$ couplings, the PFG and the nongradient HMBC maps were acquired with 8192 scans per t_1 increment (Figures 1, parts c and d, respectively). Although all cross peaks due to $^3J(^1H_\beta-^{13}C_\alpha)$ were easily attainable, three-bond connectivities linking the pyrrole β-H to the *meso*-C atoms were not detectable under the experimental conditions used thus far. The absence of the $^3J(^1H_\beta-^{13}C_{meso})$ couplings suggests that they may be different from the ^2J- or $^3J(^1H_\beta-^{13}C_\alpha)$ couplings due to unfavorable coupling pathways and/or dihedral angles or to the nature of the *meso* substituents. Work is currently in progress in our laboratory to determine if these and other heteronuclear multiple-bond correlations can be observed.

When the gradient (Figure 1b,c) and nongradient maps of **1** (Figure 1d) are compared, it is quite evident that the PFG experiment is indeed the superior experimental version for obtaining long-range couplings of **1**. When the phase-cycled map was recorded under spectral conditions identical with those used for the PFG map (1024 scans per FID), cross peaks due to $^2J_{CH}$ or $^3J_{CH}$ could not be distinguished from the noise level. To obtain reliable cross peak information from the nongradient experiment, it was necessary to acquire the map with 8192 scans per t_1 increment, which significantly prolongs the measuring time. Even under these conditions, it is still difficult to discern the desired cross peaks from the noise level (Figure 1d).

Although we have not yet obtained all three-bond couplings required for the unambiguous hyperfine shift assignments of this iron porphyrin complex, we have convincingly shown that it is advantageous to use pulsed-field gradients for the determination of long-range ^{1}H−^{13}C couplings of molecules with extremely rapidly relaxing spin systems, in spite of the lengths of the gradient pulses and the reduced spectral sensitivity. We have further demonstrated that PFG HMBC allows weak cross peak responses to be detected, which are not obtainable by conventional ^{13}C-detected NMR methods. Thus, the gradient-enhanced HMBC experiment promises to aid in the unambiguous hyperfine shift assignments of paramagnetic molecules, thereby providing a critical tool for determining the molecular and electronic structures of model hemes and other paramagnetic complexes.

Acknowledgment. The authors thank F. A. Walker (University of Arizona), A. Deese (UC San Diego), and J. V. Z. Krevor (SFSU) for helpful comments and the National Science Foundation (Grant DUE 9451624) and the National Institutes of Health (Grant DK 31038) for support of this research.

IC960797O

(21) Bax, A.; Summers, M. F. *J. Am. Chem. Soc.* **1986**, *108*, 2093.
(22) The pulsed-field gradient HMBC map was acquired with the pulse sequence available in the Bruker pulse sequence library according to ref 3c.
(23) Simonis, U.; Tan, H.; Lin, Q.; Skidmore, K.; Louie, L. Manuscript in preparation.